RSC Advances

ROYAL SOCIETY OF CHEMISTRY

www.rsc.org/advances

Journal Name

RSCPublishing

COMMUNICATION

Hybrid Fibers with Substantial Filler Contents through Kinetically Arrested Phase Separation of Liquid Jet

Cite this: DOI: 10.1039/xoxxoooooox

Jizhou Fan,[†1] Jianzhao Liu,[†1] Adam J. P. Bauer,[†1] Chananate Uthaisar,[‡] Tingying Zeng,[⊥] Chao Wang,[‖] Mingqiang Zhang,[‖] Gregory Fahs,[‖] Alan Esker,[‖] Robert B. Moore,[‖] Feng Gao,[Δ] Bingbing Li[†]*

Received ooth January 2012,
Accepted ooth January 2012

DOI: 10.1039/xoxxoooooox

www.rsc.org/

Abstract. This study reports polyhedral oligomeric silsesquioxane (POSS)-based hybrid fibers of architectural hierarchy and compositional heterogeneity. The kinetic arrest of substantial POSS content in the fibers was attributed to rapid solvent evaporation that retarded the phase separation of liquid jet. It provides new insight into the design of novel heterogeneous materials.

Polymeric materials of structural hierarchy and compositional heterogeneity have attracted wide interest for their potential applications as biomaterials,[1] photoelectronics,[2] energy storage devices,[3] and surface coatings.[4,5] Strategies employed to prepare such materials focus mainly on either controlling intermolecular interactions and therefore the nano/microscale assemblies[6] or engineering materials through three-dimensional patterning.[7] Electrospinning, a simple yet versatile technique, has great potential for developing hierarchical materials by manipulating parameters[8,9] that can control the electrospinning process under non-equilibrium conditions. Strategies that have been employed to introduce structural hierarchy and compositional heterogeneity into electrospun fibers include co-axial electrospinning to produce core-sheath or hollow fibers[10–12] and manipulating the non-equilibrium phase behavior of polymer-based blends or mixtures.[8,9,13]

In this study, poly(ε-caprolactone)(PCL)/polyhedral oligomeric silsesquioxane (1-propylmethacrylate)-heptaisobutyl substituted (m-iBuPOSS, **Fig. S1**) hybrid fibers with interesting nanopapilla and wrinkled surface features were successfully electrospun from 10:0 to 5:5 by mass PCL/m-iBuPOSS solutions with a fixed PCL concentration of 10 wt% (See Materials and Methods in Supporting Information). Here, PCL, one of the FDA-approved biodegradable and biocompatible polyesters, was used as the matrix polymer. The reactive m-iBuPOSS can be potentially used for incorporating multi-functionality into composite fibers for biomedical applications. It is worth mentioning that uniform POSS-filled fibers have been previously reported for only low loadings of POSS as traditional nanofillers.[14,15] In contrast, this study reports hybrid fibers with substantial POSS loadings up to 50 wt% (i.e., 5:5 by mass PCL/m-iBuPOSS blend). Here, the low-surface-energy m-iBuPOSS was used as an essential modulator for the phase separation of the liquid jet along the radial direction. The m-iBuPOSS surface segregation was coupled with rapid solvent evaporation that "froze" PCL chains in the outmost layer prior to drying of the inner phase, which eventually gave rise to a unique fiber architecture composed of a POSS-rich composite crust and a PCL-rich inner phase. When the POSS-rich crust was removed with hexane, the fiber architecture was clearly revealed through a combination of X-ray photoelectron spectroscopy (XPS), Raman spectroscopy, and X-ray diffraction (XRD). In comparison to previously reported composite fibers, in which nanostructures were usually used as low-loading nanofillers to achieve compositional uniformity, the PCL/POSS hybrid fibers with substantially high POSS contents reported here exhibit morphological uniformity, structural integrity, architectural hierarchy, and compositional heterogeneity. This study further demonstrates the multifaceted applications of the electrospinning technique for building heterogeneous, hierarchical materials. More importantly, it provides new insight into the effect of rapid solvent evaporation coupled with surface-directed phase separation in the liquid jet and its implications on designing novel heterogeneous materials.

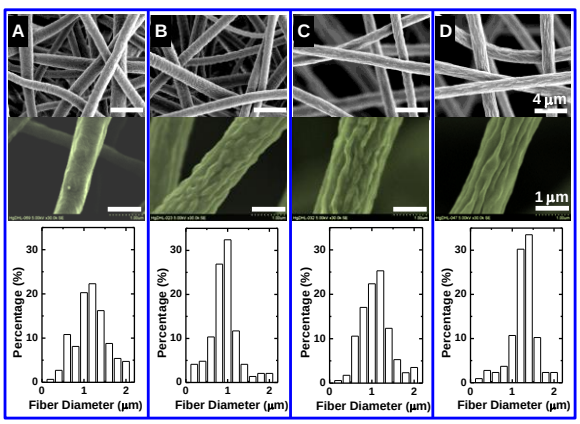

Fig. 1 SEM images of hybrid fibers electrospun from solutions with PCL/m-iBuPOSS mass ratios of (A) 10:0, (B) 8:2, (C) 7:3, and (D) 5:5, along with the histograms of fiber-size distributions. Scale bars in SEM images are 4 μm (top row) and 1 μm (second row).

As seen in the SEM images in **Fig. 1**, bead-free, uniform fibers were obtained for all electrospinning solutions with PCL/m-iBuPOSS mass ratios ranging from 10:0 (neat PCL) to 5:5. SEM images of different magnifications in **Fig. S2** further demonstrate the morphological uniformity and structural integrity of the as-spun fibers. The centers of the fiber size distributions lie between 1 and 2 μm regardless of the PCL/m-iBuPOSS mass ratios. In addition, the high-resolution SEM images in **Fig. 1A-1D** reveal that the secondary surface features (e.g., nanopapillae and wrinkles) on the fiber surfaces evolve when m-iBuPOSS content is increased. Closer examination of these secondary features shows that they are interconnected and oriented along the long axis of the hybrid fibers. In comparison to neat PCL fibers, the PCL/m-iBuPOSS fibers are more extendable and can be easily stretched to form well-aligned fibers (**Fig. S3**). The SEM images in **Fig. 2**, taken for stretched fibers, clearly reveal small raft-like domains evolving from the ridges of the aligned nanowrinkles. These raft-like domains are shown to arrange longitudinally along the fibers (highlighted by small green arrows in **Fig. 2**). **Fig. 2A'** highlights the onset of necking for the fibers under strain, suggesting that the raft-like domains originated from the ridges of the nanowrinkles. In order to further understand the architecture of these morphologically uniform and structurally intact hybrid fibers, a combination of XPS, Raman spectroscopy, and X-ray diffraction was employed to unveil the complex fiber architecture in relation to the composition. The results are discussed below.

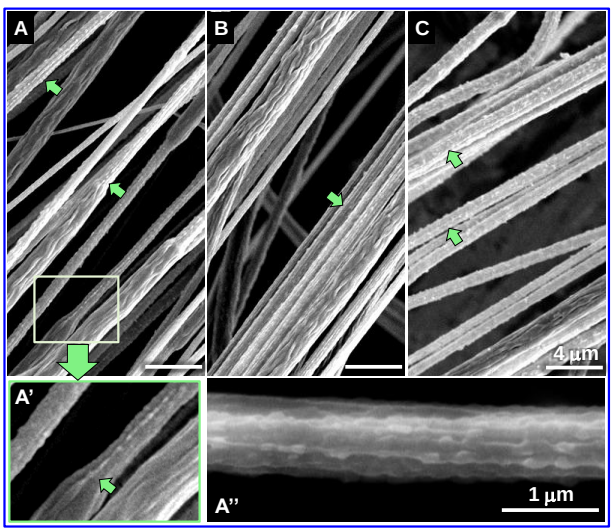

Fig. 2 SEM images of hybrid fibers electrospun from solutions with PCL/m-iBuPOSS mass ratios of (A, A', and A'') 7:3, (B) 6:4, and (C) 5:5, and stretched to twice their original lengths. The secondary features are highlighted by arrows. Scale bars for images (A-C) are 4 μm versus 1 μm for image (A'').

For the as-spun PCL/-m-iBuPOSS hybrid fibers, the incorporation of m-iBuPOSS was confirmed by both Raman spectra and XRD patterns. For instance, characteristic Raman peaks associated with C=C bond (1638 cm^{-1}) and Si-C (1331 cm^{-1}) in the methacrylic substitute groups of m-iBuPOSS[16,17] exhibit increased intensities when the m-iBuPOSS content is increased in the electrospinning solutions and therefore in the as-spun fibers [**Fig. 3A (a, b)** and **Fig. S4A**]. The increase in the intensity of absorption at 1638 cm^{-1} with the POSS content also implies that the electrospinning conditions adopted in this study do not interrupt the nonpolar C=C bond in the methacrylic substitute groups of m-iBuPOSS. Meanwhile, in addition to the peaks typical of crystalline PCL at diffraction angles (2θ) = 21.5 and 23.9°, the X-ray diffractogram of the PCL/m-iBuPOSS fibers shows additional peaks with 2θ = 8.28, 11.1, 11.7, and 19.2° [**Fig. 3B (a, b)** and **Fig. S2B**], which are similar to those previously reported for a hexagonal POSS crystal structure,[18] suggesting the existence of crystalline POSS in the as-spun hybrid fibers. The intensities of the POSS diffraction peaks also increase as the m-iBuPOSS content increases in the hybrid fibers. Thus far, a substantial amount of m-iBuPOSS, up to 50 wt%, was found to be successfully incorporated into the as-spun fibers that were structurally intact even when uniaxially stretched to twice their original lengths. However, this observation appears contradictory to what we have learned from conventional nanoparticle-filled polymer films and bulks, in which the thermodynamic incompatibility between polymer matrices and nanofillers could lead to severe phase separation and the growth of micrometer-scale POSS crystals (e.g., > 20 wt%).[19] Thus, the intact fiber morphological and spectral results presented above warrant further investigation.

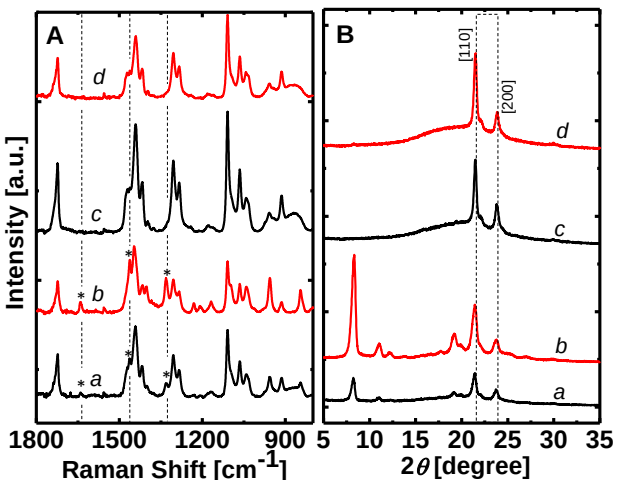

Fig. 3 Raman spectra (A) and X-ray diffraction patterns (B) of the as-spun (a, b) and the hexane-washed (c, d) fibers electrospun from (a, c) 8:2 and (b, d) 5:5 by mass PCL/m-iBuPOSS solutions.

As m-iBuPOSS could preferentially segregate at the air/fiber interface, hexane solvent that can selectively dissolve m-iBuPOSS was used to wash the as-spun fibers. The as-spun fibers were merged and shaken in hexane-filled containers for 4 days. Raman and XRD spectra for the hexane-washed fibers were then collected and are shown in **Fig. 3**. The characteristic Raman peaks associated with m-iBuPOSS (e.g., C=C at 1638 cm^{-1} and Si-C at 1331 cm^{-1}) disappeared [**Fig. 3A (c, d)**]. Furthermore, the X-ray diffraction peaks typical of m-iBuPOSS crystals were also diminished [**Fig. 3B (c, d)**]. Thus, the spectral results support that m-iBuPOSS is the major constituent of the outmost layer of the as-spun hybrid fibers. Meanwhile, the SEM images show that the hexane-washed hybrid fibers still exhibit structural integrity (**Fig. S5**).

Table 1 Atomic concentrations determined by XPS and the calculated surface compositions of the PCL/m-iBuPOSS fibers.

PCL/m-iBuPOSS (by mass)	Atomic Concentration (%)			Surface Composition (wt%)	
	Si	O	C	m-iBuPOSS	PCL
Neat PCL (control)	--	24.6	75.4	--	100
8:2	**9.86**	24.0	66.2	73.3	26.7
5:5	**10.1**	22.4	67.5	74.7	25.3
m-iBuPOSS (cal.)	**14.0**	24.6	61.4	100	--
Samples washed by hexane					
8:2	**7.85**	24.7	67.5	59.6	40.4
5:5	**7.57**	23.0	69.4	57.6	42.4
Ideal mixtures (cal.)					
8:2	**2.49**	24.9	72.6	20.0	80.0
5:5	**6.49**	24.8	68.7	50.0	50.0

Nevertheless, neither Raman spectroscopy nor XRD are surface-sensitive methods for probing the compositions of the fiber surfaces. XPS experiments were thus performed for both the as-spun fibers and the hexane-washed fibers. **Table 1** summarizes the atomic concentrations of O, C, and Si calculated from the high-resolution spectra of C1s, O1s, and Si2p peaks (**Fig. S6** and **S7**) and the surface compositions estimated according to the Si atomic concentrations. For the as-spun hybrid fibers prepared from the solutions with PCL/m-iBuPOSS mass ratios of 8:2 and 5:5, the calculated PCL surface concentrations are ~27 wt% and 25 wt%, respectively, which are significantly higher than the estimated values for spin-coated hybrid films. For instance, for the 9:1 PCL/m-iBuPOSS by mass spin-coated film, the m-iBuPOSS surface concentration is approximately 100 wt% due to the severe surface segregation of POSS (**Fig. S9**). Previous studies have clearly shown that the deposition rate of electrospun fibers can be on the order of several tens of meters per second and that the elongation rate of the liquid jet can reach up to 10^4 s^{-1}.[20, 21] Thus, the surface-area-to-volume ratio increases dramatically within milliseconds,[21] leading to very rapid solvent evaporation during electrospinning. The higher PCL surface concentrations observed for the as-spun hybrid fibers may arise from the rapid solvent evaporation during electrospinning, whereby a PCL/m-iBuPOSS composite layer could be quickly locked onto the outer surface of the drying liquid jet. Therefore, it becomes evident that the rapid solvent-evaporation process can suppress the progression of phase separation occurring in the outmost layer of the drying liquid jet, which then enables the kinetic arrest of substantial amounts of POSS (e.g., 50 wt%) into the hybrid fibers while still maintaining structural integrity and morphological uniformity of these as-spun hybrid fibers. In contrast, the spin-coated films exhibit heterogeneous surface morphology (**Fig. 4A** and **4B**), arising from severe m-iBuPOSS surface segregation followed by vertical phase separation.

Moreover, the XPS results obtained for the hexane-washed fibers still show the presence of Si on the fiber surface, even though the atomic Si concentration is decreased (**Table 1**). However, the m-iBuPOSS in the hexane-washed fibers was not detectable by less surface-sensitive methods (i.e., Raman and XRD). Therefore, the combination of Raman, XRD, and XPS studies strongly suggest that (1) the outmost m-iBuPOSS-rich composite layer of the as-spun fibers must have been washed away by the hexane, (2) the remaining m-iBuPOSS detected by XPS must mainly reside near the surface of the hexane-washed fibers, (3) the hexane-washed fibers are rich in PCL, and (4) a PCL-rich phase must exist in the inner phase of the as-spun hybrid fibers. Thus, the phase separation along the radial direction of the electrospun fibers must have occurred in the PCL/m-iBuPOSS liquid jet upon solvent evaporation during electrospinning.

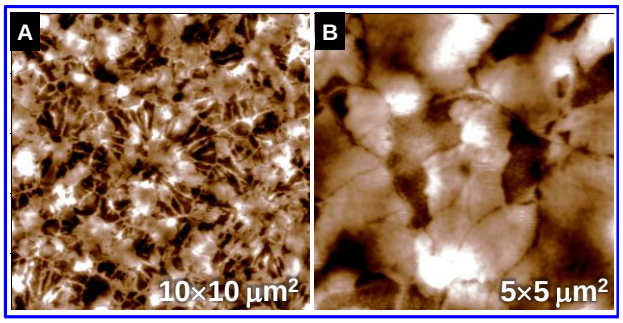

Fig. 4 Atomic force microscopy height images of hybrid thin films spin coated from 5 wt% solutions with PCL/m-iBuPOSS mass ratios of (A) 95:5 and (B) 90:10.

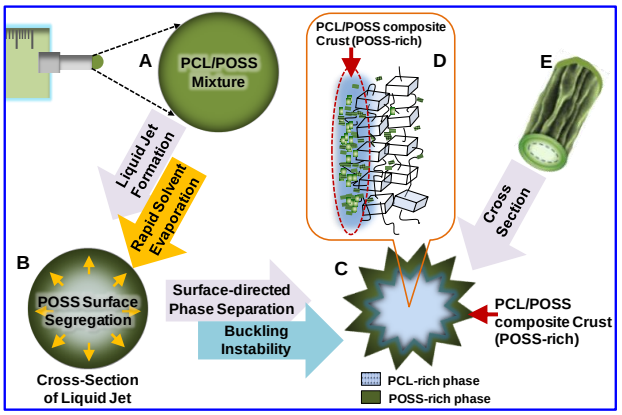

Fig. 5 Schematic illustration of the fiber-formation mechanism.

The phase separation of the binary liquid jet during electrospinning generally follows the spinodal decomposition mechanism instead of nucleation and growth since nucleation is usually slower than the initial growth of unstable concentration fluctuations in spinodal decomposition.[22] The rapid solvent evaporation also prevents further coarsening of phase-separated regions, leading to finer structures in electrospun fibers. The morphological evolution of the PCL/m-iBuPOSS hybrid fiber is illustrated schematically in **Fig. 5**. The preferential migration of low-surface-energy m-iBuPOSS to the air/jet interface, serves as the driving force for the initial surface segregation of m-iBuPOSS molecules (**Fig. 5B**). Meanwhile, the initial radial concentration gradient of the outermost layer of the liquid jet was kinetically controlled by rapid solvent evaporation. Upon rapid solvent evaporation, the PCL/m-iBuPOSS composite filled with kinetically arrested POSS was "frozen" in the dried outer surface of the liquid jet, while the inner PCL-rich phase was still drying. The mechanical mismatch between the dried, outmost POSS-rich composite layer and the wet PCL-rich inner phase provided a driving force for buckling instabilities, somewhat similar to that reported for polystyrene systems,[23] resulting in the growth of nanopapilla and nanowrinkle morphologies observed in the PCL/m-iBuPOSS hybrid fibers (**Fig. 5C**). The orientation of the wrinkles along the fiber axis can be attributed to the stretching force exerted on the drying liquid jet during electrospinning (**Fig. 5E**). Overall, in comparison to the phase separation that occurred vertically in the PCL/m-iBuPOSS spin-coated films, the phase separation that occurred in the outmost surface of the drying liquid jet was kinetically suppressed due to the rapid solvent evaporation. The retarded progression of surface-directed phase separation therefore enabled the formation of a PCL/m-iBuPOSS composite crust, giving

rise to structurally intact and morphologically uniform hybrid fibers with substantially high loadings of the m-iBuPOSS nanocages, which otherwise cannot be achieved.

Conclusions

This study reported the electrospun hybrid PCL/POSS fibers with substantially high POSS contents (e.g., 50 wt%). These hybrid fibers are of morphological uniformity, structural integrity, and architectural hierarchy, which were not expected on the basis of previous understandings of the phase behaviours of POSS-filled bulk and film systems. In contrast, the phase separation that occurred in the outer surface of the drying liquid jet was kinetically arrested due to the rapid solvent evaporation, leading to the formation of a structurally protective PCL/m-iBuPOSS composite crust. The radial phase-separation-induced compositional heterogeneity of the hybrid fibers was also made evident by analyzing the XRD, Raman, and XPS results. The current study not only significantly extends the previous understanding of POSS-filled polymer bulk and thin-film systems but also provides unique insight into the radial phase separation of the electrospinning liquid jet and its implications on the design of novel heterogeneous composite materials.

Notes and references

†Department of Chemistry, ‡Department of Physics, Science of Advanced Materials Doctoral Program, Central Michigan University, Mount Pleasant, MI 48859
‖Department of Chemistry, Virginia Tech, Blacksburg, VA 24061
⊥Research Laboratory for Electronics, Massachusetts Institute of Technology, Cambridge, MA 02139
ΔDepartment of Applied Physics, Shandong Agricultural University, Shandong, China 271018
[1]First three authors contributed equally to this manuscript.
*Corresponding Author: Bingbing Li
Department of Chemistry, Science of Advanced Materials Doctoral Program, Central Michigan University, 201 E Ottawa Ct. Dow 350, Mt. Pleasant, MI 48859
Phone: 989-774-3441
Email: li3b@cmich.edu
Fax: 989-774-3883.

Electronic Supplementary Information (ESI) available: [details of any supplementary information available should be included here]. See DOI: 10.1039/c000000x/

1 J. Tan, W. M. Saltzman, *Biomaterials*, 2004, **25**, 3593.
2 N. Kinadjian, M.-F. Achard, B. Julián-López, M. Maugey, P. Poulin, E. Prouzet, and R. Backov, *Advanced Functional Materials*, 2012, **22**, 3994.
3 A. Magasinski, P. Dixon, B. Hertzberg, A, Kvit, J. Ayala, and G. Yushin, *Nature Materials*, 2010, **9**, 353.
4 S. S. Latthe, A. L. Demirel, *Polymer Chemistry*, 2013, 4, 246.
5 K. Liu, X. Yao, and L. Jiang, *Chemical Society Reviews*, 2010, **39**, 3240.
6 Y.-C. Lin, S.-W. Kuo, *Polymer Chemistry*, 2012, **3**, 882; Z. Ren, R. Zhang, F. Wang and S. Yan, *Polymer Chemistry*, 2011, **2**, 608; Z. Ren, Y. Tian, P. Xie, S. Yan and R. Zhang, *Polymer Chemistry*, 2010, **1** , 1095.
7 J. Yom, S. M. Lane, and R. A. Vaia, *Soft Matter*, 2012, **8**, 12009.
8 P. Lu, Y. Xia, *Langmuir*, 2013, **29**, 7070.
9 S. Megelski, J. Stephens, D. B. Chase, and J. F. Rabolt, *Macromolecules*, 2002, **35**, 8456.
10 J. T. McCann, D. Li, and Y. Xia, *Journal of Material Chemistry*, 2005, **15**, 735.
11 Z. Sun, E. Zussman, A. Yarin, J. Wendorff, and A. Greiner, *Advanced Materials*, 2003, **15**, 1929.
12 J. Wu, N. Wang, Y. Zhao, and L. Jiang, *Journal of Materials Chemistry A*, 2013, **1**, 7290.
13 A. J. Bauer, T. Zeng, J. Liu, C. Uthaisar and B. Li, *Macromolecular Rapid Communications*, 2014, **35**, 715.
14 E. S. Cozza, O. Monticelli, and E. Marsano, *Macromolecular Materials and Engineering*, 2010, **295**, 791.
15 L. Gardella, A. Basso, M. Prato, and O. Monticelli, *ACS Applied Materials & Interfaces*, 2013, **5**, 7688.
16 A. Lungu, N. M. Florea, G. Voicu, and H. Iovu, *U. P. B. Sci. Bull., Series B*, 2011, **73**, 177.
17 W. Y. Chen, K. S. Ho, T. H. Hsieh, F. C. Chang, and Y. Z. Wang, *Macromolecular Rapid Communications*, 2006, **27**, 452.
18 A. J. Waddon, E. B. Coughlin, *Chemistry of materials*, 2003, **15**, 4555.
19 J. Yu, Z. Qiu, *ACS Applied Materials & Interfaces*, 2011, **3**, 890; H. Pan, J. Yu, Z. Qiu, *Polymer Engineering and Science*, 2011, **51**, 2159.
20 M. Bognitzki, T. Frese, M. Steinhart, A. Greiner, J. H. Wendorff, A. Schaper, M. Hellwig, *Polymer Engineering and Science*, 2001, **41**, 982.
21 M. Bognitzki, W. Czado, T. Frese, A. Shaper, M. Hellwig, M. Steinhart, A. Greiner, A.; J. H. Wendorff, *Advanced Materials*, 2001, **13**, 70.
22 M. Peng, D. Li, J. Shen, Y. Chen, Q. Zheng, H. Wang, *Langmuir*, 2006, **22**, 9368.
23 C.-L. Pai, M. C. Boyce, G. C. Rutledge, *Macromolecules*, 2009, **42**, 2102.